

1 Identification and characterization of *PsFwC9* conferring
2 Fusarium Wilt Resistance in Pea

3 Dong Deng ^{1,2}, Wenqi Wu ¹, Canxing Duan¹, Feng ming², Renfeng Xue², Weide Ge², Suli Sun ^{1,*}
4 & Zhendong Zhu ^{1,*}

5 ¹ Key Laboratory of Grain Crop Genetic Resources Evaluation and Utilization, Institute of Crop
6 Sciences, Chinese Academy of Agricultural Sciences, Beijing 100081, P. R. China

7 ² Crop Research Institute, Liaoning Academy of Agricultural Sciences, Shenyang, 110161, P. R.
8 China

9 * Corresponding authors E-mails: sunsuli@caas.cn (Suli Sun); zhuzhendong@caas.cn (Zhendong
10 Zhu)

11
12
13
14
15
16
17
18
19
20
21
22
23
24
25
26
27
28
29
30
31
32
33
34
35 © The Author(s) 2026. Published by Oxford University Press on behalf of the Nanjing
36 Agricultural University. This is an Open Access article distributed under the terms of the
37 Creative Commons Attribution License <https://creativecommons.org/licenses/by/4.0/>,
38 which permits unrestricted reuse, distribution, and reproduction in any medium, provided
39 the original work is properly cited.

40 Abstract

41 Pea (*Pisum sativum* L.) is one of the most important edible legumes in China, with both planting
42 area and total yield ranking among the highest in the world. Fusarium wilt, caused by *Fusarium*
43 *oxysporum* f. sp. *pisi* (*Fop*), is a severe factor limiting pea production. The deployment of
44 resistant pea cultivars is the most effective and sustainable strategy for controlling this disease.
45 In the present study, a novel resistance gene *PsFwC9*, conferring resistance to *Fop* race 5, was
46 identified in the resistant pure line Chengwan 9-8 (CW9-8), and its candidate gene
47 *Psat4g213640* was characterized and functionally validated to be associated with disease
48 resistance. Genetic analysis of the F₂ population derived from the cross between the resistant
49 parent CW9-8 and the susceptible parent Chengwan 9-1 (CW9-1) revealed that *PsFwC9* was
50 controlled by a single dominant gene. Based on whole-genome resequencing, bulked segregant
51 analysis sequencing (BSA-seq), and fine mapping, *PsFwC9* was localized to an 817.06 kb
52 region on chromosome 4 (i.e., linkage group IV, chr4LG4), flanked by KASP markers A016508
53 and A016511, and co-segregated with four markers. Haplotype analysis revealed that only the
54 marker A016615 was significantly associated with Fusarium wilt resistance, and this marker
55 was designated as a diagnostic marker for *PsFwC9*. Marker A016615 was located at
56 425,699,725 bp on chr4LG4, corresponding to the 277 bp within *Psat4g213640*, where a “G/A”
57 single-nucleotide polymorphism caused an amino acid substitution leading to an alteration in
58 protein structure, therefore *Psat4g213640* was identified as *PsFwC9* candidate gene.
59 Quantitative real-time PCR analysis showed no significant difference in the expression levels
60 of *Psat4g213640* between CW9-8 and CW9-1. Overexpression of the candidate gene
61 *Psat4g213640*^{CW9-8} in the hairy root system significantly enhanced the resistance of CW9-1 to
62 Fusarium wilt, whereas RNA interference-mediated silencing of *Psat4g213640*^{CW9-8} reduced
63 the resistance of CW9-8, indicating that *Psat4g213640*^{CW9-8} played a crucial role in pea
64 resistance to Fusarium wilt. In addition, subcellular localization showed that the protein
65 encoded by *Psat4g213640* was targeted to the endoplasmic reticulum. Collectively, these
66 findings not only enriched the gene resources for disease resistance in pea and provided an
67 important foundation for elucidating the molecular mechanism of *PsFwC9*-mediated resistance,
68 but also provided important technical support for the practical application of molecular
69 breeding for disease resistance in pea.

70 **Keywords:** *Pisum sativum*, *Fusarium oxysporum* f. sp. *psi*, fine mapping, resistance gene,
71 function characterization

72

ACCEPTED MANUSCRIPT

73 Introduction

74 Pea (*Pisum sativum* L.), comprising green and dry pea, serves as an important edible legume for
75 human consumption or animal feed, offering essential protein, carbohydrates, vitamins, dietary fiber,
76 minerals, and other bioactive compounds [1-4]. Another important property of pea is its symbiotic
77 nitrogen-fixing ability, which is one of the leading leguminous plants in agricultural systems. Since
78 the 20th century, pea has been widely grown in the world for economic return, soil fertility
79 improvement in cereal and oilseed crop rotations, as a break crop for disease control, and an
80 alternative to summer fallow [5-7].

81 However, the disease has become increasingly prominent with the expansion of pea cultivation
82 area. Fusarium wilt, caused by *Fusarium oxysporum* f. sp. *pisi* (*Fop*), is a devastating disease that
83 can severely reduce yield and quality in most pea-producing regions worldwide [8-11]. The *Fop* has
84 been physiologically differentiated into four races (1, 2, 5, and 6), and the deployment of race-
85 specific resistant cultivars remains the most economical and effective strategy for managing
86 Fusarium wilt. [10-13]. Several studies on Fusarium wilt resistance in pea have been undertaken
87 over the years, giving rise to the development of resistant cultivars tailored to different physiological
88 races for crop improvement. For example, Neumann and Xue [14] identified 49 accessions with
89 resistance to at least one physiological race, Bani et al. [15] found 20 accessions resistant to race 2,
90 and Deng et al. [10] discovered 192 accessions resistant to race 5. These resistant
91 accessions provide valuable genetic resources that can be utilized in the development of resistant
92 cultivars and integrated strategies for effective Fusarium wilt management in pea.

93 Exploring the genetic foundation of Fusarium wilt resistance is essential for the advancement
94 of pea breeding [16-18]. Genetic resistance to *Fop* races 1 [17, 19], 5 [16, 20, 21], and 6 [21] is
95 conferred by single dominant genes, and to race 2 is controlled by multiple genes [18]. Each of
96 these genes was characterized for resistance to a specific race, but several of them may also provide
97 cross-resistance to other races [16, 18]. Despite the availability of effective linkage maps, only a
98 limited number of Fusarium wilt resistance-related genes and quantitative trait loci (QTLs) have
99 been identified in pea, including the complete resistance genes *Fw* [17, 22] and *Fwf* [20, 22], as well
100 as the putative partial resistance gene *Fnw4.1* [18], which are mapped to linkage groups (LG) 3, 6,
101 and 4, respectively. In recent years, bulked segregant analysis sequencing (BSA-seq) has rapidly

102 emerged as a powerful tool for detecting candidate regions associated with resistance traits and has
103 been successfully applied to identify Fusarium wilt resistance genes in crop species, such as flax,
104 eggplant, and pea [16, 23, 24]. In pea, Deng et al. [16] employed BSA-seq analysis and fine mapping
105 to identify *Past6g003960* on chromosome 6 (linkage group II, chr6LG2) as the candidate gene for
106 the Fusarium wilt resistance gene *FwSI* in the cultivar Shijiadacaiwan 1, and further confirmed that
107 88 out of 152 resistant individuals carried the *FwSI*. Nevertheless, *FwSI* may be closely linked to
108 *Fwf* or even represent the same gene, and additional verification remains necessary [16, 20]. Besides,
109 the complex NB-ARC (nucleotide-binding adaptor shared by APAF-1, R proteins, and CED-4)
110 repeat structure of the *FwSI* candidate gene poses challenges to investigating its functional
111 characterization [16, 25, 26]. Therefore, discovering new resistance genes is essential for resistance
112 breeding and elucidating the genetic foundation of Fusarium wilt resistance in pea.

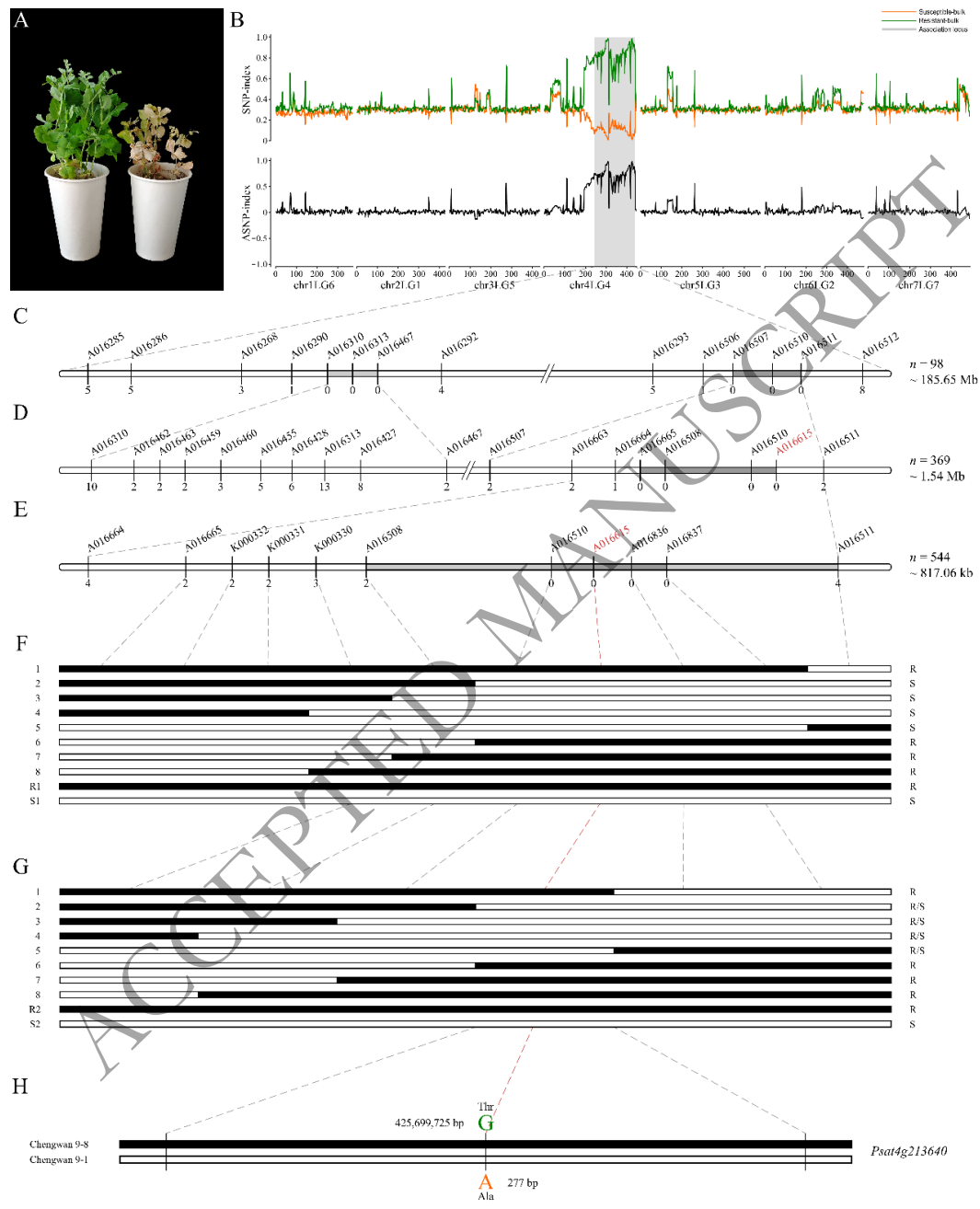
113 In China, pea is primarily grown in mountainous or hilly areas with poor soils or as a rotational
114 crop following major staple crops [4, 5, 27, 28]. In spite of these constraints, China holds the top
115 position globally in green pea production and ranks third in dry pea production [29]. However, pea
116 yields in main production regions affected by Fusarium wilt typically are reduced by 30%, with
117 severe cases leading to losses exceeding 50% or even total crop failure [5, 10, 28]. Research on
118 resistance genes and the genetic basis of Fusarium wilt resistance in China remains relatively limited.
119 Chengwan 9 is an excellent green pea cultivar bred by Sichuan Academy of Agricultural Sciences
120 in 2007. Our previous research revealed that the cultivar was segregant for Fusarium wilt resistance
121 to race 5 and did not carry the *FwSI* [16]. Hence, in this study, we employ the Fusarium wilt-
122 resistant and susceptible pure lines, Chengwan 9-8 (CW9-8, resistant) and Chengwan 9-1 (CW9-1,
123 susceptible), derived from cultivar Chengwan 9 (CW9) to construct a genetic population to explore
124 the Fusarium wilt resistance gene *PsFwC9* in Chengwan 9. Our objectives are to: (a) identify single-
125 nucleotide polymorphisms (SNPs) and Insertion-Deletions (InDels) associated with Fusarium wilt
126 resistance, (b) identify potential resistance genes within the candidate region, and (c) conduct
127 preliminary functional validation of these candidate genes.

128 **Results**

129 **Phenotypic evaluation for Fusarium wilt**

130 After 28 dpi, all seedlings of susceptible parent CW9-1 and the differential cultivars Litter

131 Marvel, Darkskin Perfection, New Era, and New Season, exhibited wilted and died, whereas the
 132 plants of resistant parent CW9-8 and the differential cultivars WSU 23, WSU 28, and WSU 31,
 133 maintained normal growth with negligible observable disease symptoms (Fig. 1A). The results
 134 confirmed that CW9-8 was resistant to *Fop* race 5.



135
 136 **Figure 1.** Bulked segregant analysis sequencing, mapping and haplotype analyses of the resistance
 137 gene *PsFwC9* against Fusarium wilt. (A) Phenotypes of the resistant parent Chengwan 9-8 (CW9-8,
 138 left) and the susceptible parent Chengwan 9-1 (CW9-1, right), (B) Mapping of the *PsFwC9* resistance
 139 locus through BSA-seq, with the x-axis indicating the physical positions of 7 pea chromosomes (in
 140 megabases, Mb), and the y-axis representing SNP-index or Δ SNP-index values. (C) The initial mapping
 141 of *PsFwC9* using 98 F₂ individuals from the cross of CW9-1 and CW9-8. (D) The mapping of *PsFwC9*

142 using 369 F₂ individuals derived from CW9-1 and CW9-8. (E) Fine mapping of *PsFwC9* using 544 F₂
 143 individuals from the cross of CW9-1 and CW9-8. In (C), (D) and (E), the numbers below the line
 144 indicated recombinants detected by the marker. (F) Genotypes and phenotypes of key recombinants in
 145 544 F₂ individuals. (G) Haplotype analysis of 218 accessions showing genotypes and phenotypes of
 146 significant recombinants. In (F) and (G), black rectangles correspond to homozygous or heterozygous
 147 genotypes of CW9-8, and white rectangles represent homozygous genotypes of CW9-1. (H) Comparison
 148 of the candidate SNP locus at KASP marker A016615 between CW9-8 and CW9-1, with the vertical line
 149 marking the nonsynonymous SNP and amino acid change. The numbers above and below the rectangles
 150 represent the position on the chromosome and gene, respectively.

151 **Table 1.** Genetic segregation in response to *Fusarium oxysporum* f. sp. *pisi* in the F₂ population
 152 derived from Chengwan 9-1 and Chengwan 9-8

| Parent and the cross | Generation | Amount | Observed number ^a | | Chi-squared tests ^b | | |
|----------------------|----------------|--------|------------------------------|----|--------------------------------|----------|----------|
| | | | R | S | Expected ratio | χ^2 | <i>P</i> |
| Chengwan 9-8 (CW9-8) | P ₁ | 30 | 30 | – | – | – | – |
| Chengwan 9-1 (CW9-1) | P ₂ | 30 | – | 30 | – | – | – |
| CW9-1 × CW9-8-A | F ₂ | 98 | 68 | 30 | 3:1 | 1.65 | 0.20 |
| CW9-1 × CW9-8-B | F ₂ | 72 | 53 | 19 | 3:1 | 0.07 | 0.79 |
| CW9-1 × CW9-8-C | F ₂ | 54 | 38 | 16 | 3:1 | 0.62 | 0.43 |
| CW9-1 × CW9-8-D | F ₂ | 72 | 58 | 14 | 3:1 | 1.19 | 0.28 |
| CW9-1 × CW9-8-E | F ₂ | 73 | 53 | 20 | 3:1 | 0.75 | 0.39 |
| CW9-1 × CW9-8-F | F ₂ | 46 | 32 | 14 | 3:1 | 0.72 | 0.39 |
| CW9-1 × CW9-8-G | F ₂ | 45 | 34 | 11 | 3:1 | 0.01 | 0.93 |
| CW9-1 × CW9-8-H | F ₂ | 55 | 39 | 16 | 3:1 | 0.49 | 0.48 |
| CW9-1 × CW9- | F ₂ | 29 | 21 | 8 | 3:1 | 0.10 | 0.74 |

| | | | | | | | |
|---------------|----------------|-----|-----|-----|-----|------|------|
| CW9-1 × CW9-8 | F ₂ | 544 | 396 | 148 | 3:1 | 1.78 | 0.18 |
|---------------|----------------|-----|-----|-----|-----|------|------|

153 ^a, R, resistant; S, susceptible. ^b, expected ratio: Dominant trait individual: Recessive trait individual
 154 = 3:1; The $\chi^2 < 3.84$ and $P > 0.05$ indicated that the theoretical segregation ratio is significantly
 155 correlated with the actual.

156 In the mapping population consisting of 544 individuals from nine CW9-1 × CW9-8 F₂
 157 populations, 396 individuals exhibited resistance (R) to *Fop* race 5 isolates PF22b, while 148
 158 individuals showed susceptibility (S), corresponding to a segregation ratio of 3:1 by the Chi-square
 159 test with $\chi^2 = 1.78$ and $p = 0.18$ (Table 1). The analysis of the nine F₂ populations also revealed a
 160 consistent 3:1 segregation ratio for resistance and susceptibility, where χ^2 values were below 3.84
 161 and p -values were greater than 0.05 (Table 1). The results indicated Fusarium wilt resistance in
 162 CW9-8 should be controlled by a single dominant gene, and named *PsFwC9*.

163 Furthermore, among the 13 other pure lines of the CW9, five lines showed resistance, whereas
 164 eight lines displayed susceptible or highly susceptible (Table S1). Leaf samples from the five
 165 resistant and eight susceptible individuals were collected for further haplotype analysis.

166 Reads mapping and BSA-seq analysis

167 Utilizing the Illumina platform and fastp v0.23.1 software, approximately 48.30 Gb, 48.89 Gb,
 168 92.22 Gb, and 89.91 Gb clean data were generated for the CW9-1, CW9-8, CW9S, and CW9R,
 169 respectively. Following the alignment of clean data to the reference genome Caméor v1a, a total of
 170 320 million and 324 million paired-end 150-bp mapped reads were obtained for parents CW9-1 and
 171 CW9-8, achieving mean depths of 14.98× and 14.81×, with 4× genome coverage rates of 74.19%
 172 and 74.04%, respectively (Table 2). For the two bulks CW9S and CW9R, 614 million and 599
 173 million paired-end 150-bp mapped reads were captured, resulting in mean depths of 25.78× and
 174 25.12×, and 4× genome coverage rates of 78.52% and 78.11%, respectively (Table 2).

175 **Table 2** Whole-genome resequencing of parents and bulks using Illumina sequencing

| Genotype sample | Clean base (Gb) | Number of clean reads | Mapping rate (%) | Mean depth (×) | 4× genome coverage rate (%) |
|-----------------|-----------------|-----------------------|------------------|----------------|-----------------------------|
| Chengwan 9-1 | 48.30 | 320,074,459 | 99.39 | 14.81 | 74.04 |

| | | | | | |
|----------|-------|-------------|-------|-------|-------|
| Chengwan | 48.89 | 324,043,762 | 99.41 | 14.98 | 74.19 |
| 9-8 | | | | | |
| CW9S | 92.22 | 610,790,390 | 99.34 | 25.78 | 78.52 |
| CW9R | 89.91 | 599,377,398 | 99.44 | 25.12 | 78.11 |

176 A total of 23,062,829 variant loci were detected on the seven crucial chromosomes of pea
 177 through comparison with the reference genome, yielding 1,713,204 reliable SNPs and InDels
 178 following continuous filtering (Table S4). In this study, InDels were regarded as SNPs to calculate
 179 and analyze the SNP-index. The SNP-index and Δ SNP-index value were calculated for each SNP
 180 loci to determine the genomic region associated with *Fop* resistance. A 201.5 Mb genomic region
 181 (243,351,840-444,788,063) on chr4LG4, showing a high average Δ SNP-index in both bulks, was
 182 speculated to be the candidate region containing *PsFwC9* (Fig. 1B). Within this extensive candidate
 183 region, two specific areas, measuring 3.88 Mb (307,291,808-311,172,916) and 3.74 Mb
 184 (424,037,046-427,779,104), exhibited an average SNP-index value greater than 0.95 for CW9R and
 185 less than 0.5 for CW9S, with Δ SNP-index values exceeding 0.9, leading to the conclusion that these
 186 locations were strongly associated with *PsFwC9* (Fig. 1B).

187 **Fine mapping of *PsFwC9***

188 According to the BSA-seq analysis and gene annotation, 40 KASP markers (Table S2) were
 189 first developed within the 201.5 Mb candidate region on chr4LG4 and used to genotype 98
 190 individuals from the CW9-1 \times CW9-8-A F₂ population. Six markers showed consistent linkage to
 191 *PsFwC9*, with A016310, A016313, and A016467 found in the 3.88 Mb (307.29 Mb-311.17 Mb)
 192 highly correlated region, while A016507, A016510, and A016511 were situated in the 3.74 Mb
 193 (424.04 Mb-427.78 Mb) closely linked region, with the two intervals separated by approximately
 194 112.87 Mb (Fig. 1C). To define the candidate region of *PsFwC9*, 20 additional KASP markers (Table
 195 S2) were developed to genotype 369 individuals from five F₂ populations (A-E) derived from CW9-
 196 1 \times CW9-8. The *PsFwC9* was delimited to an 834.79 kb interval between markers A016664 and
 197 A016511, co-segregating with markers A016665, A016508, A016510, and A016615, located within
 198 the 424.04-427.78 Mb candidate region (Fig. 1D). Subsequently, to further refine the candidate
 199 region, the mapping population was expanded to nine F₂ populations (A-I) of CW9-1 \times CW9-8,
 200 comprising 544 individuals, and 10 more KASP markers were developed for detection within this
 201 interval. The candidate region of *PsFwC9* was narrowed down to 817.06 kb, flanked by markers

202 A016508 and A016511, and the *PsFwC9* was co-segregating with markers A016510, A016615,
203 A016836, and A016837, indicating that no recombination events occurred (Fig. 1E). Moreover, the
204 544 F₂ individuals could be categorized into 10 haplotypes based on the 10 markers. The presence
205 of SNPs corresponding to markers A016510, A016615, A016836, and A016837 in individuals,
206 reliably demonstrated resistance to Fusarium wilt, whereas individuals without these five SNPs
207 presented a susceptible phenotype (Fig. 1F).

208 **Haplotype analysis and diagnostic marker of *PsFwC9***

209 The six KASP markers, either co-segregated or tightly linked with the *PsFwC9*, were utilized
210 to detect 218 pea accessions with known resistance phenotypes, aiming to determine SNPs related
211 to Fusarium wilt resistance and to discover accessions carrying the unique *PsFwC9* haplotype. A
212 total of 10 haplotypes were identified among 218 accessions, where accessions with SNP variation
213 at the marker A016615 consistently exhibited resistance to Fusarium wilt, while those without the
214 variation showed either resistant or susceptible (Fig. 1G). Some accessions containing the other
215 variations of five markers exhibited susceptibility to Fusarium wilt, indicating that these SNPs are
216 not associated with the *PsFwC9* resistance gene.

217 These findings suggest that the “A” to “G” SNP variation at marker A016615 could be a crucial
218 factor in determining pea resistance to Fusarium wilt (Fig. 1H). Although the variation at this marker
219 locus was detected in only 13 accessions (Table S1), among which six pure lines derived from CW9
220 were homozygous for the mutation (G/G) and the remaining seven accessions (including CW9 itself)
221 were heterozygous (G/A), the marker A016615 successfully identified the resistance-associated
222 allele in accessions and populations with distinct genetic backgrounds, demonstrating strong
223 specificity and stability across diverse accessions. Therefore, the KASP marker A016615 was
224 designated as the diagnostic molecular marker for the *PsFwC9* resistance gene.

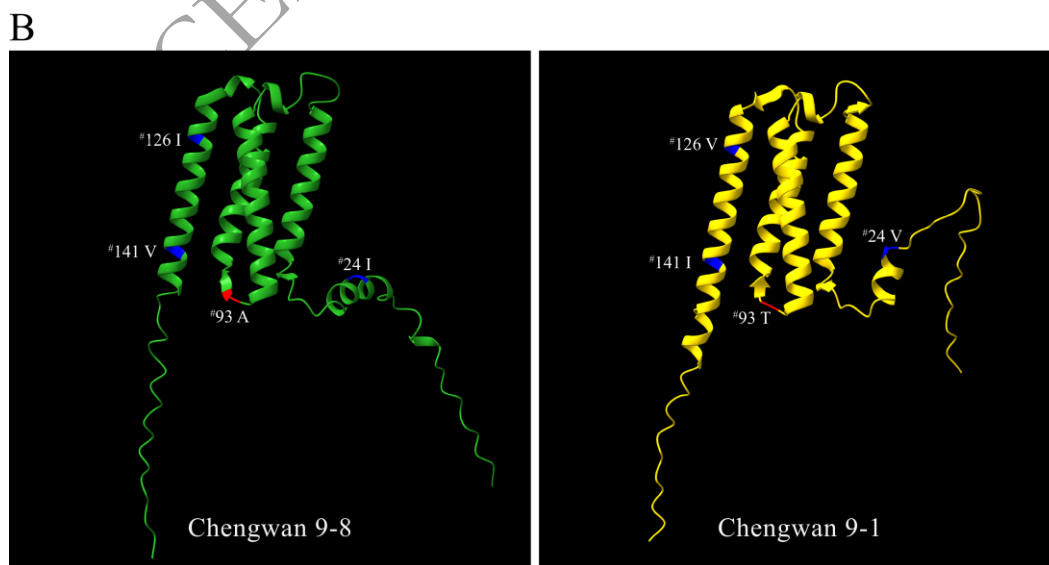
225 **Candidate gene identification of *PsFwC9***

226 Haplotype analysis revealed that marker A016615 was the only locus specifically associated
227 with the resistance gene *PsFwC9*. Based on the Caméor reference genome and sequence alignment,
228 the functional SNP, located at 425,699,725 bp on chr4LG4, corresponding to position 277 bp within
229 *Psat4g213640*, involved a “G/A” substitution, leading to an amino acid change from Threonine (Thr)
230 to Alanine (Ala). In addition, five mutation loci were identified in the *Psat4g213640* between the
231 resistant parent CW9-8 and the susceptible parent CW9-1. Among them, two were synonymous

232 substitutions, while the remaining three corresponded to the co-segregated markers within the gene,
 233 resulting in only conservative amino acid changes between valine (Val) and isoleucine (Ile) [30, 31]
 234 (Fig. 2A). These results indicate that A016615 was the only disease-resistance-associated locus and
 235 *Psat4g213640* could be candidate gene of *PsFwC9*.

A

| | | |
|-------------------------------------|--|-------------|
| Chengwan 9-8 cDNA (<i>PsFwC9</i>) | ATGGAACGATGGTAAAACCAAGATCCAAATTTAAACGTGCTTTAAGAGGTCCTAAAGTGACCATTAAATTTGTCACGTGTTTATAACATC | 90 |
| Chengwan 9-8 amino acid | M E R M V K P R S K F K R A L R G P K V T I N I V T V Y N I | 30 |
| Chengwan 9-1 cDNA | ATGGAACGATGGTAAAACCAAGATCCAAATTTAAACGTGCTTTAAGAGGTCCTAAAGTGACCATTAAATTTGTCACGTGTTTATAACATC | 90 |
| Chengwan 9-1 amino acid | M E R M V K P R S K F K R A L R G P K V T I N V V T V Y N I | 30 |
| Caméor cDNA (<i>Psat4g213640</i>) | ATGGAACGATGGTAAAACCAAGATCCAAATTTAAACGTGCTTTAAGAGGTCCTAAAGTGACCATTAAATTTGTCACGTGTTTATAACATC | 425,699,538 |
| Caméor amino acid | M E R M V K P R S K F K R A L R G P K V T I N V V T V Y N I | 30 |
| Chengwan 9-8 cDNA (<i>PsFwC9</i>) | ATGGGATTAGAACCAATTCCTCGATGGCCTTGTAGCCCTTATTTCTTTGACTACTTGGTTTCTCCCAAATTAGATATCCAGAAAT | 180 |
| Chengwan 9-8 amino acid | M G L E T N S L H G L V A F I F F V L L G F L Q I R Y P E N | 60 |
| Chengwan 9-1 cDNA | ATGGGATTAGAACCAATTCCTCGATGGCCTTGTAGCCCTTATTTCTTTGACTACTTGGTTTCTCCCAAATTAGATATCCAGAAAT | 180 |
| Chengwan 9-1 amino acid | M G L E T N S L H G L V A F I F F V L L G F L Q I R Y P E N | 60 |
| Caméor cDNA (<i>Psat4g213640</i>) | ATGGGATTAGAACCAATTCCTCGATGGCCTTGTAGCCCTTATTTCTTTGACTACTTGGTTTCTCCCAAATTAGATATCCAGAAAT | 425,699,628 |
| Caméor amino acid | M G L E T N S L H G L V A F I F F V L L G F L Q I R Y P E N | 60 |
| Chengwan 9-8 cDNA (<i>PsFwC9</i>) | CCTACCCCATTTTCAGCACCATCCAAAGACAACATTAGTATCCATTGCTAGTTTCTACTATATGTTTGGCTTTTGGTTAAGCTTAAG | 270 |
| Chengwan 9-8 amino acid | P T P F Q H H P K T T L V S I A S F L L Y C L A F W V K L K | 90 |
| Chengwan 9-1 cDNA | CCTACCCCATTTTCAGCACCATCCAAAGACAACATTAGTATCCATTGCTAGTTTCTACTATATGTTTGGCTTTTGGTTAAGCTTAAG | 270 |
| Chengwan 9-1 amino acid | P T P F Q H H P K T T L V S I A S F L L Y C L A F W V K L K | 90 |
| Caméor cDNA (<i>Psat4g213640</i>) | CCTACCCCATTTTCAGCACCATCCAAAGACAACATTAGTATCCATTGCTAGTTTCTACTATATGTTTGGCTTTTGGTTAAGCTTAAG | 425,699,718 |
| Caméor amino acid | P T P F Q H H P K T T L V S I A S F L L Y C L A F W V K L K | 90 |
| Chengwan 9-8 cDNA (<i>PsFwC9</i>) | TTTGAAACAAGGGTTGATACCTTCATGGAAGTGTGGTTCACCTTCATTGGTTTCCTTAGGTTGATGTTGTTACCAGACAAGTGGGAA | 360 |
| Chengwan 9-8 amino acid | F E A R V D T F M E V F G S L S L V S L V L M L L P D K W E | 120 |
| Chengwan 9-1 cDNA | TTTGAAACAAGGGTTGATACCTTCATGGAAGTGTGGTTCACCTTCATTGGTTTCCTTAGGTTGATGTTGTTACCAGACAAGTGGGAA | 360 |
| Chengwan 9-1 amino acid | F E I R V D T F M E V F G S L S L V S L V L M L L P D K W E | 120 |
| Caméor cDNA (<i>Psat4g213640</i>) | TTTGAAACAAGGGTTGATACCTTCATGGAAGTGTGGTTCACCTTCATTGGTTTCCTTAGGTTGATGTTGTTACCAGACAAGTGGGAA | 425,699,808 |
| Caméor amino acid | F E I R V D T F M E V F G S L S L V S L V L M L L P D K W E | 120 |
| Chengwan 9-8 cDNA (<i>PsFwC9</i>) | TTATTGGATACATTATCATATATTCATATGTTTATTTGCCATGTAATGTTATGTCGACTTTGTTTATTTGGGTTACGTCCAAAA | 450 |
| Chengwan 9-8 amino acid | L F G Y I I I Y S I W F I C H V I V M V V L C F I G L R P K | 150 |
| Chengwan 9-1 cDNA | TTATTGGATACATTATCATATATTCATATGTTTATTTGCCATGTAATGTTATGTCGACTTTGTTTATTTGGGTTACGTCCAAAA | 450 |
| Chengwan 9-1 amino acid | L F G Y I V I Y S I W F I C H V I V M V I L C F I G L R P K | 150 |
| Caméor cDNA (<i>Psat4g213640</i>) | TTATTGGATACATTATCATATATTCATATGTTTATTTGCCATGTAATGTTATGTCGACTTTGTTTATTTGGGTTACGTCCAAAA | 425,699,898 |
| Caméor amino acid | L F G Y I V I Y S I W F I C H V I V M V I L C F I G L R P K | 150 |
| Chengwan 9-8 cDNA (<i>PsFwC9</i>) | TTGAAGAGGTGCCACCACCTTGGCAATCTCAATTGATTTGAACTAA | 501 |
| Chengwan 9-8 amino acid | L K R L P P L L P N T S I D L N * | 166 |
| Chengwan 9-1 cDNA | TTGAAGAGGTGCCACCACCTTGGCAATCTCAATTGATTTGAACTAA | 501 |
| Chengwan 9-1 amino acid | L K R L P P L L P N T S I D L N * | 166 |
| Caméor cDNA (<i>Psat4g213640</i>) | TTGAAGAGGTGCCACCACCTTGGCAATCTCAATTGATTTGAACTAA | 425,699,949 |
| Caméor amino acid | L K R L P P L L P N T S I D L N * | 166 |



236
 237 **Figure 2.** Comparison of DNA and amino acid sequences (A) and predicted protein structures (B)

238 of the candidate gene *Psat4g213640* among Chengwan 9-8 and Chengwan 9-1. (A) The cDNA
239 sequence of the candidate gene is completely consistent with the corresponding genomic DNA sequence
240 in the reference genome. (B) The Numbers indicate amino acid positions, and single-letter codes
241 represent amino acid residues.

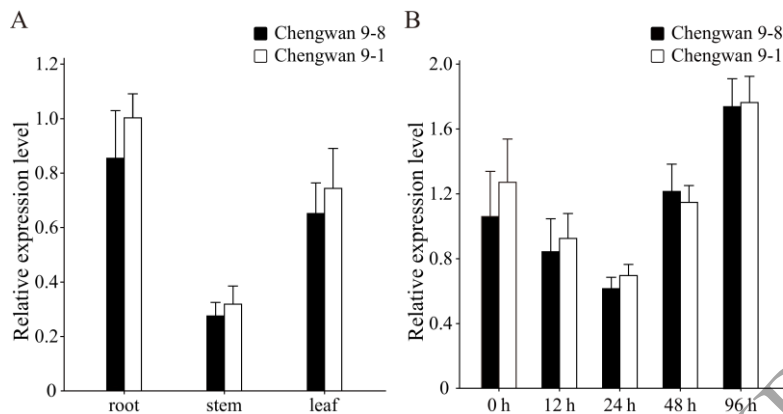
242 The predicted protein structures of *Psat4g213640*^{CW9-8} and *Psat4g213640*^{CW9-1} exhibited a
243 similar overall fold, both consisting of three α -helices in the N-terminal region followed by an
244 extended C-terminal coil (Fig. 2B). Nevertheless, subtle conformational distinctions were observed.
245 The C-terminal region of *Psat4g213640*^{CW9-1} appeared slightly more extended, whereas
246 *Psat4g213640*^{CW9-8} displayed a more compact and inward-bent configuration. Moreover, four amino
247 acid substitutions were identified between the two proteins: Ile-24-Val, Ala-93-Thr, Ile-126-Val, and
248 Val-141-Ile. Among them, the Ala-93-Thr replacement, located near the loop connecting α -helices,
249 results in the loss of a hydroxyl group and potential hydrogen bonds, likely affecting local structural
250 stability or interactions with other membrane-associated components. The remaining substitutions
251 represented conservative hydrophobic exchanges that might have fine-tuned helix packing but were
252 unlikely to cause major structural rearrangements.

253 **Expression patterns of *PsFwC9***

254 In order to verify the correlation between the candidate gene and Fusarium wilt resistance,
255 qRT-PCR analysis was conducted to examine the expression pattern of *Psat4g213640* in the
256 susceptible parent CW9-1 and the resistant parent CW9-8. The expression levels of *Psat4g213640*
257 were examined by qRT-PCR in the roots, stems, and leaves of CW9-8 and CW9-1 at the seedling
258 stage. Specifically, the *Psat4g213640* exhibited the highest expression in roots and the lowest in
259 stems in both parents, but no significant difference in expression levels was observed between CW9-
260 8 and CW9-1 in any of the tested tissues (Fig. 3A).

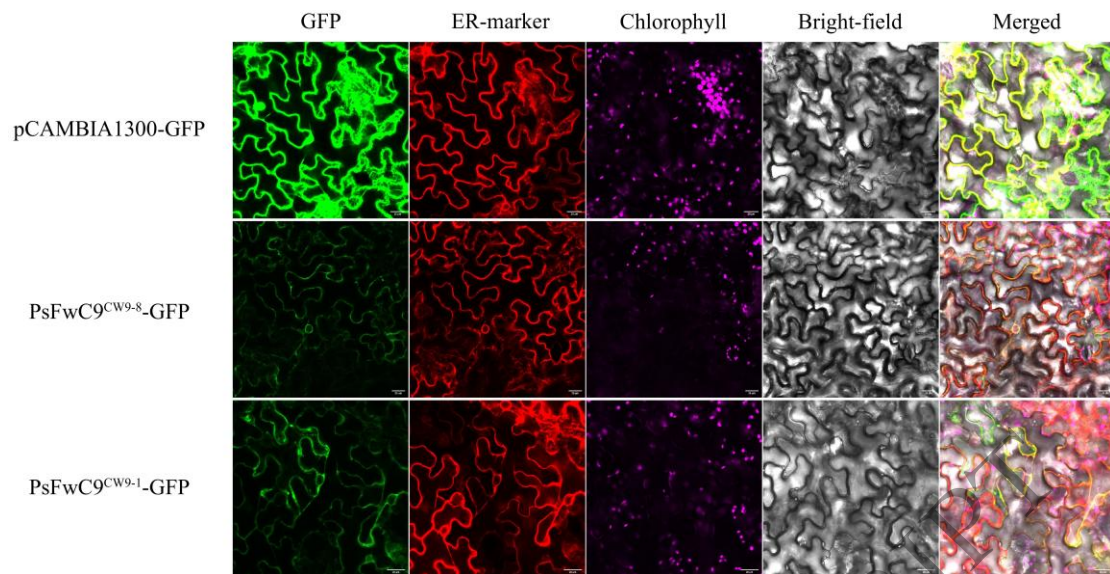
261 Subsequently, the expression of *Psat4g213640* in the roots of pea seedlings was quantitatively
262 analyzed at five different time points after inoculation. The results showed that the expression
263 patterns of *Psat4g213640* were similar between the two parental lines. Both parental lines exhibited
264 a similar temporal expression pattern of *Psat4g213640* after inoculation, with transcript levels
265 decreasing initially and reaching the lowest point at 24 h, followed by a gradual increase that peaked
266 at 96 h. No significant differences in *Psat4g213640* expression were observed between the two
267 parents at any of the tested time points (Fig. 3B). Therefore, these results suggested that the

268 Fusarium wilt resistance in CW9-8 might be not associated with the expression level of the
 269 candidate gene *Psat4g213640*.



270
 271 **Figure 3.** Expression patterns of *PsFwC9* candidate gene *Psat4g213640*. (A) Expression patterns of
 272 *Psat4g213640* in roots, stems, and leaves of Chengwan 9-8 and Chengwan 9-1. (B) Relative expression
 273 levels of *Psat4g213640* in the roots of Chengwan 9-8 and Chengwan 9-1 at 0, 12, 24, 48 and 96 h after
 274 inoculation with *Fusarium oxysporum* f. sp. *pisi*. In (A) and (B), the qRT-PCR results were normalized
 275 to the expression of reference gene *PsActin*, and values were presented as the mean (\pm standard error) of
 276 three independent replicates.

277 To determine the subcellular localization of the *PsFwC9* candidate gene, the coding sequence
 278 of *Psat4g213640* was fused to GFP to generate the *PsFwC9*^{CW9-8}-GFP and *PsFwC9*^{CW9-1}-GFP
 279 construct. The recombinant vector was transiently expressed in epidermal cells of *Nicotiana*
 280 *benthamiana* via *Agrobacterium tumefaciens* strain GV3101. Confocal microscopy showed that the
 281 control GFP signal was distributed throughout the cytoplasm and nucleus, whereas the *PsFwC9*^{CW9-}
 282 ⁸-GFP and *PsFwC9*^{CW9-1}-GFP fluorescence displayed a typical reticular pattern and was mainly
 283 observed in the endoplasmic reticulum (ER), with weak signals detected at the plasma membrane
 284 (Fig. S1). Co-localization analysis with an ER marker showed that the GFP signal overlapped
 285 strongly with the ER marker, confirming that *PsFwC9* is localized to the endoplasmic reticulum
 286 (Fig. 4).



287

288 **Figure 4.** Subcellular colocalization of *PsFwC9* candidate gene *Psat4g213640* in *Nicotiana*
 289 *benthamiana* leaves.

290 **Functional validation of *Psat4g213640* in Fusarium wilt resistance**

291 Due to the lack of an efficient genetic transformation system in pea, a hairy root system was
 292 used to investigate the role of the *PsFwC9* candidate gene *Psat4g213640*^{CW9-8} in Fusarium wilt
 293 resistance. The overexpression construct *PsFwC9*-OE was introduced into *Agrobacterium*
 294 *rhizogenes* strain K599 to induce hairy roots in the susceptible parent CW9-1. Vigorously growing
 295 hairy roots were selected for expression analysis and PAS staining.

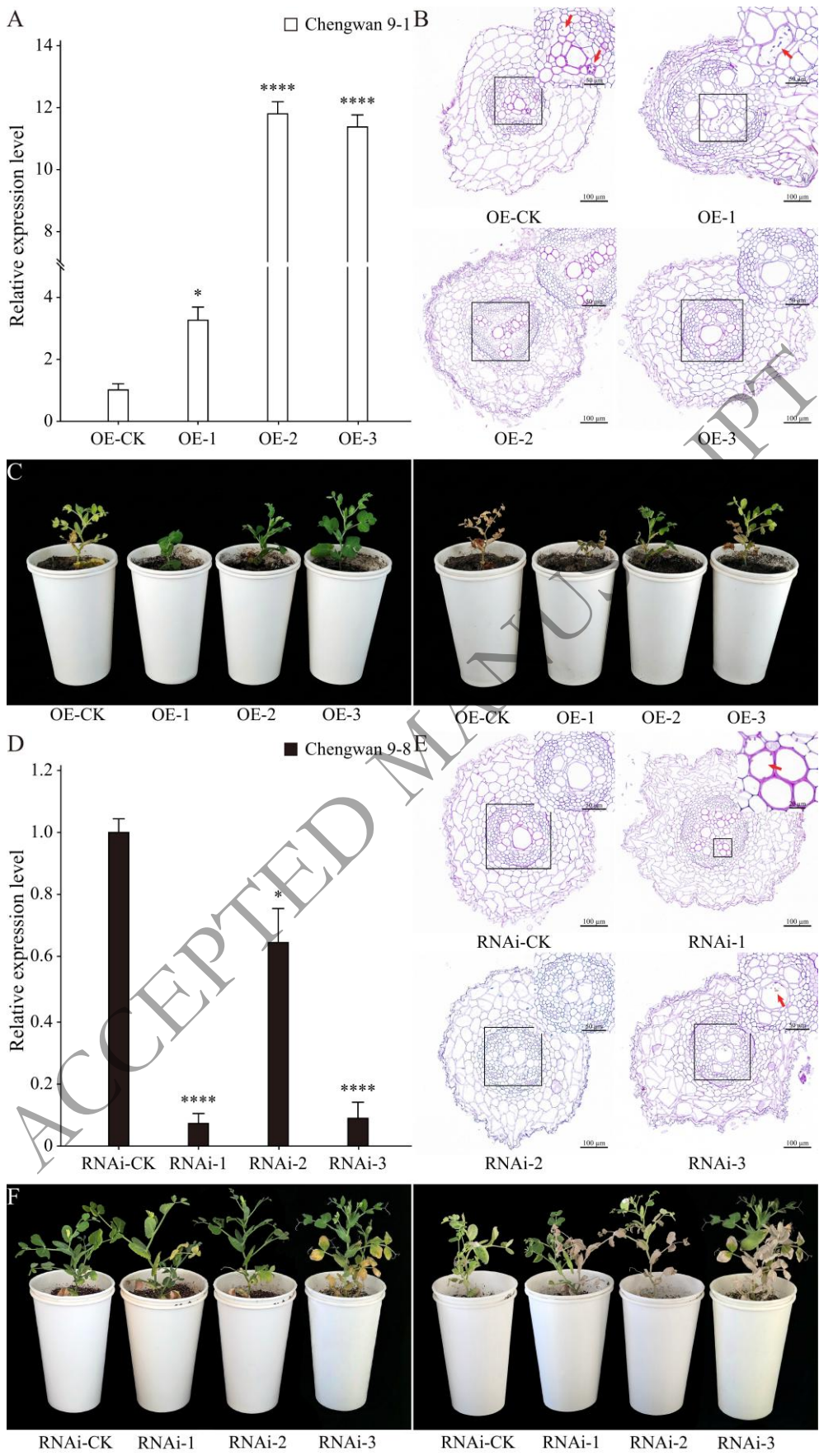
296 The qRT-PCR analysis revealed that the expression levels of *Psat4g213640* in the hairy roots
 297 of the overexpression lines CW9-1_OE-1, CW9-1_OE-2, and CW9-1_OE-3 were significantly
 298 higher than those in the control, with expression levels increased by 3.2-, 11.8-, and 11.3-fold,
 299 respectively. The differences were statistically significant ($P < 0.05$) and highly significant ($P <$
 300 0.0001) (Fig. 5A). PAS staining of the overexpression hairy roots showed that at 24 h post
 301 inoculation, *Fop* microconidia had invaded the vascular tissues of both the control and CW9-1_OE-
 302 1 roots, whereas no *Fop* microconidia were observed in the vascular tissues of CW9-1_OE-2 and
 303 CW9-1_OE-3 roots (Fig. 5B). The visible disease symptoms appeared in the control plants at 10
 304 dpi, whereas no obvious symptoms were observed in CW9-1_OE-1, CW9-1_OE-2 or CW9-1_OE-
 305 3 plants. At 18 dpi, both the control and CW9-1_OE-1 plants had completely wilted, whereas CW9-
 306 1_OE-2 and CW9-1_OE-3 plants exhibited only mild wilting symptoms and survived until
 307 approximately 30 dpi, when complete wilting eventually occurred (Fig. 5C). These results indicated

308 that overexpression of *Psat4g213640* enhanced resistance to Fusarium wilt., effectively delaying
309 the onset of disease symptoms and extending seedling survival.

310 RNA interference (RNAi) analysis was subsequently performed in the resistant parent CW9-8
311 using the same hairy root system. The qRT-PCR results showed that the expression levels of
312 *Psat4g213640*^{CW9-8} in the hairy roots of the RNAi lines CW9-8_RNAi-1, CW9-8_RNAi-2, and
313 CW9-8_RNAi-3 were reduced to 7.3%, 64.9%, and 8.9% of the control levels, respectively,
314 showing highly significant ($P < 0.0001$) and significant ($P < 0.05$) differences (Fig. 5D). PAS
315 staining at 24 h post inoculation revealed that a small number of *Fop* microconidia had invaded the
316 vascular tissues of CW9-8_RNAi-1 and CW9-8_RNAi-3 roots, whereas no fungal spores were
317 observed in the control or CW9-8_RNAi-2 roots (Fig. 5E). At 18 dpi, CW9-8_RNAi-1 and CW9-
318 8_RNAi-3 plants showed early wilting symptoms, characterized by leaf chlorosis, whereas no
319 visible symptoms were observed in the control or CW9-8_RNAi-2 plants. At 40 dpi, all plants
320 remained alive; however, one branch of both CW9-8_RNAi-1 and CW9-8_RNAi-3 had completely
321 wilted, and approximately half of the leaves on CW9-8_RNAi-2 displayed chlorosis and wilting
322 symptoms. The disease index of CW9-8_RNAi plants increased significantly, while the control
323 plants showed only natural senescence of basal leaves (Fig. 5F). These results indicated that RNAi-
324 mediated silencing of *Psat4g213640* compromised resistance to Fusarium wilt.

325 Taken together, these results demonstrate that *Psat4g213640* played a positive role in resistance
326 to Fusarium wilt in pea.

ACCEPTED MANUSCRIPT



327

328 **Figure 5.** Overexpression and RNA interference of *PsFwC9* candidate gene *Psat4g213640* in hairy

329 roots. (A) and (D) showed the expression levels of *Psat4g213640* in the best growing hairy root of
330 overexpression and RNA interference, respectively. the qRT-PCR results were normalized to the
331 expression of reference gene *PsActin*, and values were presented as the mean (\pm standard error) of three
332 independent replicates. ‘*’ and ‘****’ indicate significant differences at the 0.05 and 0.0001 levels,
333 respectively. (B) and (E) were the Periodic Acid-Schiff staining results of the vigorously growing hairy
334 root of overexpression and RNA interference, respectively. (C) and (F) were the phenotypic evaluation
335 of overexpression and RNA interference at different times after inoculation, respectively.

336 Discussion

337 The pea Fusarium wilt caused by *Fop* is a destructive vascular disease that results in severe
338 yield losses and continues to be a major constraint to pea production worldwide [9-11]. The
339 deployment of resistant cultivars is widely recognized as the most economical, efficient, and
340 environmentally sustainable strategy for controlling Fusarium wilt [10, 11, 15]. Therefore,
341 identifying Fusarium wilt resistance genes in pea and clarifying their genetic characteristics are
342 essential for the innovation, utilization, and molecular breeding of resistant cultivars [16-18].
343 However, *F. oxysporum* can gain virulence to overcome single-gene resistance through mutation or
344 horizontal gene transfer, suggesting that breeding strategies relying solely on individual resistance
345 genes carry potential risks [32-35]. The identification and functional validation of new resistance
346 genes are vital for enriching resistance resources and addressing these challenges, providing more
347 genetic options for pea breeding and enabling gene pyramiding strategies to enhance resistance
348 durability and reduce the risk posed by pathogen variability [36, 37]. Therefore, the CW9-8, an elite
349 pea pure line carrying new resistance gene to Fusarium wilt, was selected for fine mapping and
350 functional characterization of the resistance gene, aiming to provide a novel gene and diagnostic
351 marker for Fusarium wilt resistance breeding in pea, as well as new insights into the underlying
352 mechanisms of resistance.

353 The BSA method is an effective method for rapidly identifying trait-associated markers by
354 constructing DNA bulks from individuals displaying extreme phenotypes [38]. With the
355 advancement of next-generation sequencing technologies and the release of reference genomes for
356 multiple crops, it is now possible to efficiently detect high-throughput SNPs and InDels related to
357 target traits by combining whole genome resequencing with BSA [39, 40]. Peas have a significantly

358 lower propagation rate compared to gramineous crops like rice, wheat, and maize, making it difficult
359 to fine mapping target genes using traditional mapping techniques [41-43]. Unlike traditional
360 methods that require large genetic populations, the BSA-seq technique can efficiently identify
361 candidate regions and molecular markers associated with target traits by sequencing and analyzing
362 bulks from a limited number of extreme individuals, and this approach has been successfully utilized
363 for identifying many traits in pea, such as disease resistance [16, 44], stress tolerance [45], and
364 morphological traits [46, 47]. In this study, the candidate region associated with resistance to
365 Fusarium wilt was identified using the BSA-seq technique. Following this, the resistance gene
366 *PsFwC9* was finely mapped using traditional linkage analysis, along with an expanded mapping
367 population, which narrowed the candidate region to 817.06 kb with four co-segregating markers.
368 The strategy of combining BSA-seq with traditional mapping methods accelerated the identification
369 of the *PsFwC9* candidate gene, which could be utilized for gene mapping of target traits in peas and
370 other crops as well.

371 Previous studies have reported several Fusarium wilt resistance genes in pea, including *Fw* on
372 chr5LG3 conferring resistance to *Fop* race 1 [17, 19], *Fwf* on chr6LG2 providing resistance to race
373 5 [20, 22], and *Fnw4*, a major-effect gene on chr4LG4 associated with resistance to race 2 [21].
374 More recently, the resistance gene *FwSI* was identified on chr6LG2 within a 91.4 kb region and
375 was proposed to confer resistance to race 5, with genetic evidence suggesting that *FwSI* may be
376 closely linked to, or even identical with, the previously reported *Fwf* locus [16]. In this study,
377 haplotype analysis revealed that only marker A016615 was associated with Fusarium wilt resistance,
378 and the locus corresponding to this marker was identified as 277 bp of the gene *Psat4g213640* on
379 chr4LG4 in the pea reference genome. Sequence comparison between the resistant parent CW9-8
380 and the susceptible parent CW9-1 revealed six SNP variations in *Psat4g213640*. Among them, the
381 SNP corresponding to marker A016615 involved an A-to-G substitution, resulting in an amino acid
382 change from Thr (a polar amino acid) to Ala (a nonpolar amino acid). The remaining five variations
383 consisted of conservative substitutions between Val and Ile or synonymous mutations, which were
384 less likely to substantially affect protein function [30, 31]. Notably, the candidate gene
385 *Psat4g213640* differed from the previously reported *FwSI* candidate gene *Psat6g003960* located
386 on chr6LG2. Sequence analysis of *Psat6g003960* revealed the presence of a typical NB-ARC
387 domain, a conserved functional ATPase module widely found in classical plant resistance proteins

388 and known to regulate resistance-protein activation. In contrast, *Psat4g213640* lacked recognizable
389 resistance-related domains and showed no clear functional annotation in the Caméor v1a and
390 Zhongwan 6 v1.0 reference genomes or in public databases such as NCBI
391 (<https://www.ncbi.nlm.nih.gov/>) or TAIR (<https://www.arabidopsis.org/>). The structural and
392 genomic differences between these genes suggested that *PsFwC9* might represent a distinct
393 resistance locus from the previously reported *FwS1* or *Fwf* region and might contribute to Fusarium
394 wilt resistance through a mechanism different from classical NB-ARC type resistance proteins.
395 Based on the combined evidence from fine mapping, haplotype analysis, and sequence comparison,
396 *Psat4g213640* was considered candidate gene underlying *PsFwC9*. In addition, the SNP represented
397 by marker A016615 could serve as a diagnostic marker for the precise identification of the *PsFwC9*
398 allele in different pea populations and germplasm resources. To our knowledge, this study provides
399 the first evidence of a Fusarium wilt resistance gene candidate located on pea chr4LG4.

400 Gene expression analysis is a commonly used approach to verify target gene function. Among
401 these methods, qRT-PCR has become one of the most widely applied techniques for measuring gene
402 expression levels owing to its superior accuracy and sensitivity [48-50]. In qRT-PCR, gene
403 expression quantification can be performed using either absolute or relative quantification methods
404 [49, 51, 52]. Since absolute quantification requires converting data into absolute copy numbers, a
405 process that is often unnecessary in practical research [51], relative quantification has become the
406 more widely adopted approach due to its simplicity and practicality [49, 50, 52]. In this study, the
407 expression of the candidate gene *Psat4g213640* was quantitatively analyzed using qRT-PCR. The
408 results showed that *Psat4g213640* was expressed in the roots, stems, and leaves of both parents,
409 with the highest expression in roots. After *Fop* inoculation, the expression patterns of *Psat4g213640*
410 in both parents exhibited similar trends and no significant differences were detected, suggesting that
411 the resistance of CW9-8 might not be directly linked to the expression level of *Psat4g213640*, but
412 rather was granted by alterations in its protein structure or function, since amino acid substitutions
413 could modify the protein ability to interact with pathogen effectors or activate downstream defense
414 signaling pathways, thereby influencing the plant resistance to disease [53-56].

415 The *Agrobacterium rhizogenes*-mediated hairy root transformation provides a powerful
416 transient gene expression system for studying root biology and has been successfully applied to
417 more than 100 plant species, including soybean and common bean [50, 57, 58, 59]. This technique

418 enables researchers to rapidly obtain transgenic hairy roots, allowing efficient functional
419 characterization of genes, particularly those involved in root development, nutrient uptake, and
420 stress responses. Moreover, the hairy root system circumvents the complexity and time consumption
421 associated with conventional transgenic technologies, offering a practical platform for root-specific
422 gene function analysis in crops that lack an established stable transformation system [57, 59]. Gene
423 overexpression and gene silencing are two complementary strategies for functional gene validation.
424 Overexpression enhances the transcriptional level of the target gene to assess the potential gain of
425 function under elevated expression, whereas gene silencing reduces gene expression to investigate
426 the phenotypic or functional consequences of expression suppression [50, 53]. In this study, the
427 hairy root system was employed to perform overexpression and gene silencing experiments of the
428 candidate gene *Psat4g213640*. Overexpression of *Psat4g213640^{CW9-8}* significantly enhanced the
429 resistance of the susceptible parent CW9-1 to Fusarium wilt, delaying disease onset and progression,
430 indicating that this gene conferred resistance in CW9-1. In contrast, RNAi of *Psat4g213640^{CW9-8}*
431 markedly reduced the resistance of the resistant parent CW9-8, further confirming that
432 *Psat4g213640^{CW9-8}* is a key gene underlying Fusarium wilt resistance in CW9-8. It should be noted
433 that due to the presence of untransformed roots or insufficient efficiency of overexpression and
434 silencing in *Agrobacterium rhizogenes*-induced hairy root systems, the expression levels of some
435 transformed roots showed no significant differences from the controls, leading the overall plant
436 resistance to gradually approach its original phenotype [50, 53, 57, 59]. Nevertheless, this study not
437 only verified the critical role of *Psat4g213640^{CW9-8}* in Fusarium wilt resistance but also
438 demonstrated that the hairy root system served as a reliable tool for investigating root-associated
439 gene functions. Future studies could improve the accuracy and reproducibility of this approach by
440 optimizing transformation efficiency and screening strategies.

441 Protein structure prediction serves as a fundamental basis for elucidating biological function
442 [50, 53, 55]. In this study, the predicted structural comparison revealed that *Psat4g213640^{CW9-1}* and
443 *Psat4g213640^{CW9-8}* shared a similar overall fold but exhibited subtle differences, including a slightly
444 more extended C-terminal region in *Psat4g213640^{CW9-1}* and four amino acid substitutions (Ile-24-
445 Val, Ala-93-Thr, Ile-126-Val, and Val-141-Ile). Among these, the Ala-93-Thr substitution located
446 near the loop connecting α -helices might influence local structural stability and flexibility, thereby
447 affecting protein-protein interactions. Threonine residues contain a hydroxyl group capable of

448 participating in hydrogen bonding and phosphorylation-related interactions, whereas substitution
449 with alanine removes this functional group and may disrupt local stabilizing interactions within α -
450 helices or adjacent structural elements [60-62]. Similar Thr-to-Ala substitutions have been shown
451 to alter protein stability or conformational dynamics by modifying hydrogen-bond networks or helix
452 capping interactions. For example, mutation of Thr-101Ala in the nitrate transporter NRT1.1 has
453 been demonstrated to change its functional state and transport activity through phosphorylation-
454 dependent structural regulation [62, 63]. In addition, structural studies of proteins such as
455 thioredoxin have indicated that Thr-to-Ala substitutions can weaken helix stability and alter packing
456 interactions, thereby affecting protein conformational flexibility [60, 64]. These observations
457 suggest that the amino acid substitutions identified in *Psat4g213640*, particularly the Thr-to-Ala
458 change, may influence local structural stability or protein interactions, which could ultimately
459 contribute to the functional differences observed between resistant and susceptible lines. Further
460 biochemical and structural studies will be required to determine how the amino acid substitutions
461 influence the structure and activity of *PsFwC9*.

462 Subcellular localization analysis is a crucial step for further elucidating protein function, as the
463 intracellular localization of a protein is closely associated with its biological role [53, 55]. In this
464 study, subcellular localization analysis showed that the protein encoded by *Psat4g213640* was
465 predominantly localized to the endoplasmic reticulum, suggesting that it may participate in plant
466 defense responses through ER-associated signaling regulation or protein processing. The
467 endoplasmic reticulum is an important cellular compartment responsible for protein synthesis,
468 folding, and trafficking, and it plays a crucial role in plant immune responses. Many immune-related
469 proteins undergo folding and maturation in the endoplasmic reticulum before being transported to
470 the plasma membrane or other cellular compartments, where they participate in pathogen
471 recognition and signal transduction [65-67]. In addition, the endoplasmic reticulum is closely
472 associated with intracellular Ca^{2+} signaling, reactive oxygen species (ROS) production, and stress
473 responses [68-71]. Therefore, the ER-localized *PsFwC9* may contribute to resistance against
474 *Fusarium* wilt in pea by regulating the processing and transport of immune-related proteins or by
475 participating in ER-associated defense signaling pathways. Future studies could further explore the
476 functional mechanisms of *Psat4g213640*^{CW9-8} by combining transient and stable transformation
477 systems, transcriptomic profiling, and protein to protein interaction assays to validate its role in

478 membrane-associated defense signaling.

479 **Conclusion**

480 In summary, this study provided significant insights into the genetic basis of Fusarium wilt
481 resistance in pea. A novel Fusarium wilt resistance gene, *PsFwC9*, in pea line CW9-8 was finely
482 mapped through BSA-Seq analysis, and candidate gene *Psat4g213640* was identified by haplotype
483 analysis and gene cloning. The qRT-PCR analysis showed that *Psat4g213640* was expressed in
484 multiple tissues of both resistant and susceptible parents, but its expression level was not
485 significantly correlated with resistance. Protein structure prediction revealed that the amino acid
486 substitution at the *Psat4g213640* altered the overall conformation of the protein. Subcellular co-
487 localization confirmed that the *Psat4g213640*-encoded protein was localized to the endoplasmic
488 reticulum. Functional validation using the hairy root transformation system demonstrated that
489 overexpression of *Psat4g213640*^{CW9-8} significantly enhanced resistance to Fusarium wilt in the
490 susceptible line CW9-1, whereas RNAi-mediated silencing of *Psat4g213640*^{CW9-8} in the resistant
491 line CW9-8 markedly reduced its resistance. Collectively, these findings indicate that *PsFwC9* is a
492 key gene conferring Fusarium wilt resistance in pea, and the locus and molecular markers identified
493 herein provide a solid foundation for future molecular breeding and genetic improvement of
494 Fusarium wilt resistance in pea.

495 **Materials and methods**

496 **Plant materials and pathogen inoculum**

497 The heterozygous resistant cultivar CW9 was acquired from Sichuan Academy of Agricultural
498 Sciences (SAAS) in 2019. Then, 15 pure lines were developed from CW9 through continuous single
499 plant selection and Fusarium wilt identification for three consecutive years. Among these, the
500 purified resistant line CW9-8 was used as the paternal parent, and the purified susceptible line CW9-
501 1 as the maternal parent, to construct a F₂ population for BSA-seq analysis and fine mapping.
502 Moreover, seven differential cultivars for race identification of *Fop* (Litter Marvel, Darkskin
503 Perfection, New Era, New Season, WSU 23, WSU 28, and WSU 31) obtained from the United States
504 Department of Agriculture, Agricultural Research Service (USDA ARS) were used as contrasting
505 controls. The 196 accessions with known resistance responses from the China National Crop
506 Genebank were employed for haplotype analysis (Table S1) [16].

507 The *Fop* race 5 isolate PF22b, obtained from Jianyang City, Sichuan Province, was employed
508 for phenotypic evaluations [10]. This isolate was stored at -80°C for long-term preservation and
509 cultured on potato dextrose agar (PDA) medium at 27°C for experimental use.

510 **Phenotypic evaluation for Fusarium wilt**

511 Nine F₂ populations derived from CW9-1 × CW9-8, consisting of 542 individual seeds were
512 planted sequentially in paper cups (600 mL) filled with fresh vermiculite. Approximately 150 plants
513 with 30 parental lines were grown in each sowing batch. Each paper cup was planted with five seeds,
514 and the cups were placed in greenhouses with 24-26°C for two weeks. The seedlings were inoculated
515 with *Fop* race 5 isolate PF22b using a modified root-dipping inoculation method described by Bani
516 et al. [15] and Deng et al. [10, 16]. Briefly, small mycelial plugs were cut from the edges of 7-day-
517 old fungal colonies and placed into pea broth medium, then shaken at 120 rpm and 27°C for two
518 days. After filtration, the microconidia suspension was adjusted to a final concentration of 1.0 ×
519 10⁷ microconidia/mL. Seedlings were uprooted from vermiculite, washed, and the bottom third of
520 the roots was trimmed. The remaining roots were dipped in the microconidia suspension for 3 min
521 before being transplanted in new paper cups. The control seedlings underwent the same process,
522 with sterile water substituted for the microconidia suspension. The inoculated seedlings were grown
523 under natural light in greenhouses at 27°C for an additional 28 days, with watering as needed.
524 Disease severity was assessed based on the percentage of symptomatic leaves (PSL) for individual
525 seedling following the method of Deng et al. [10, 16], where the PSL between 0 and 50 indicated
526 the seedlings were resistant, while values between 50 and 100 signified susceptible.

527 **Construction of extreme bulks and Illumina sequencing**

528 Leaf samples from both parental lines and individual plants were collected two days post-
529 inoculation (dpi) seedlings, and their genomic DNA was extracted using the DNAsure Plant Kit
530 DP320-03 (Tiangen Biotech, Beijing, China), according to the manufacturer's instructions. The
531 DNA quality and concentration of each sample were detected using 1% agarose gel electrophoresis
532 and a NanoDrop 2000/2000c spectrophotometer (Thermo Fisher Scientific, Waltham, MA, USA),
533 respectively. Following phenotypic evaluation, the DNA samples from 15 extreme resistant and 15
534 extreme susceptible seedlings in CW9-1 × CW9-8 - A F₂ population were combined to create a
535 resistant bulk (CW9R) and a susceptible bulk (CW9S), respectively. The two bulks, CW9R and
536 CW9S, along with the parents, CW9-8 and CW9-1, were sent to Novogene (Tianjin, China) for

537 construction of Illumina libraries and whole-genome resequencing (WGRS), with the bulks
538 sequenced at 20× coverage, and the parents at 10× coverage.

539 **Identification of genomic region responsible for Fusarium wilt resistance**

540 The clean data reads were obtained after removing paired-end reads with low quality ($Q < 15$),
541 low-length reads (< 20 bp), more than 5 undetermined bases, and adapter sequences in raw data
542 reads by fastp v0.23.4 software [72]. The high-quality reads were aligned to pea genome reference
543 sequences Caméor v1a (<https://urgi.versailles.inra.fr/Species/Pisum>) using bwa-mem2 v2.2.1
544 software [73, 74]. The alignment results were then sorted and filtered for accurate reads using
545 samtools v1.18 software [75], while GATK v4.4.0 [76] was applied to mark and remove duplicate
546 reads, as well as to calculate the mapping rate, 4× genome coverage, and mean depth. The SNPs
547 and InDels were detected using GATK HaplotypeCaller [76, 77], vcftools v0.1.16 software [78],
548 and Linux commands, based on the following criteria: (1) variations present in all samples; (2)
549 homozygous variations in parental samples; (3) variations loci on major chromosomes with
550 sequencing depth $\geq 4\times$.

551 The high-quality differential SNPs and insertion-deletion (InDel) sites were identified
552 following the filtering process. The SNP-index, defined as the ratio of reads containing SNPs and
553 InDels to the total number of reads, was calculated for the CW9R and CW9S [39]. The Δ SNP-index,
554 representing the difference in SNP-index values between the two bulks, was used to identify
555 candidate genomic regions associated with disease resistance. Each locus in the Δ SNP-index was
556 calculated by subtracting the SNP-index of the CW9R from that of the CW9S, following this
557 formula:

$$558 \quad \Delta\text{SNP-index} = \frac{\text{Alt}_R}{\text{Alt}_R + \text{Ref}_R} - \frac{\text{Alt}_S}{\text{Alt}_S + \text{Ref}_S}$$

559 where R = the CW9R, S = the CW9S, Ref = the read depth matching that of the reference
560 genome, and Alt = the read depth deviating from that of the reference genome. The values of two
561 SNP-indexes and Δ SNP-index was visualized with QTL-seq v2.2.3 software [40] and Adobe
562 Illustrator 2025 (<http://www.adobe.com>). A higher Δ SNP-index indicates a stronger likelihood that
563 the SNPs and InDels were involved in *Fop* resistance or were linked to a gene regulating this trait.

564 In defining the candidate region, the absence of QTLs at that position was assumed, resulting
565 in the random allocation of locus genotyping between the two progenies during genetic evaluation.

566 The SNPs and InDels with Δ SNP-index ≥ 0.75 were selected for annotation with SnpEff v5.2
567 software [79]. The available genomic annotation files (gff/gtf,
568 <https://urgi.versailles.inra.fr/Species/Pisum>) were utilized to determine the genomic locations and
569 mutation types of SNPs and InDels.

570 **Marker development and fine mapping**

571 The non-significant SNP and InDel loci were filtered out according to the gene annotation, and
572 the retained loci with 200 bp flanking sequences on both sides were extracted using TBtools-II
573 v2.027 software [80]. A local BLAST was then conducted to align these extracted sequences with
574 the reference genome Caméor v1a, excluding sequences with more than four copies in the genome.
575 The SNP and InDel loci within the target genomic region were chosen for conversion into
576 Kompetitive Allele-Specific PCR (KASP) markers using the Polymarker online platform
577 (<http://www.polymarker.info/>). All KASP primers and subsequent primers were synthesized by
578 Sangon Biotech (Shanghai, China).

579 The 5' end of both forward primers in each designed KASP assay was modified by adding the
580 standard FAM-label or HEX-label fluorescent sequence (FAM tail: 5'-
581 GAAGGTGACCAAGTTCATGCT-3'; HEX tail: 5'-GAAGGTCGGAGTCAACGGATT-3') (Table
582 S2). The amplification of KASP markers was performed on a Douglas Scientific Array Tape
583 Platform (China Golden Marker, Beijing) in a 1.6 μ L reaction volume, containing 0.8 μ L DNA (~22
584 ng/ μ L), 0.022 μ L primer mix, 0.4 μ L KASP V4.0 2 \times Mastermix 1536 (LGC Biosearch Technologies,
585 Shanghai, China), and 0.4 μ L ddH₂O. PCR amplification was conducted on a Soellex PCR Thermal
586 Cycler (Douglas Scientific, Alexandria, MN, USA) with the following protocol: an initial
587 denaturation at 94°C for 15 minutes, followed by 10 touchdown cycles of 94°C for 20 s and 65°C
588 for 1 min (decreasing by 0.6°C each cycle), then 26 cycles of 94°C for 20 s and 55°C for 1 min,
589 concluding with a final cooling step at 4°C. Fluorescent end-point readings were performed using
590 the Araya fluorescence detection system (integrated with the Douglas Scientific Array Tape
591 Platform), and genotypes and clusters were visualized with Kraken2 v2.0.8 software [81].
592 Sequential evaluation of the F₂ populations was conducted using KASP markers. Candidate genes
593 were identified based on co-segregating markers, while markers with more than 5% recombination
594 events in the same population would be removed. Then, the genetic physical maps of KASP markers
595 linked to the Fusarium wilt resistance gene were generated through Adobe Illustrator 2025.

596 **Candidate gene identification and diagnostic marker verification**

597 The KASP markers associated with the candidate region was utilized to genotype the 218 pea
598 individuals with known phenotypes (Table S1). Markers associated with genotypes in susceptible
599 individuals that correspond to those of the resistant parent would be removed. The applicable
600 markers were utilized as diagnostic markers for the detection of the gene in pea accessions. The
601 candidate resistance gene could be refined to those linked with these diagnostic markers. The
602 diagnostic markers developed were also validated using individual plants from the CW9 pea lines.

603 **Candidate gene cloning and sequence alignment**

604 Candidate gene *Psat4g213640* identified through haplotype analysis were further analyzed by
605 sequence alignment. The primers *PsFwC9*-gene-F/R were designed with NCBI primer designing
606 tool (<https://www.ncbi.nlm.nih.gov/tools/primer-blast/>) to amplify *Psat4g213640* from the parental
607 lines CW9-1 and CW9-8 (Table S2). The PCR amplification was completed through a TC-E-480
608 thermocycler (Bioer Technology, Hangzhou) in 40 μ L reaction mixtures: containing 4 μ L genomic
609 DNA (~ 20 ng/ μ L), 1.6 μ L of each primer, 20 μ L of 2 \times Taq PCR Master Mix (Tiangen Biotech,
610 Beijing, China), and 12.8 μ L ddH₂O. The thermal cycling conditions were 94 $^{\circ}$ C for 5 min; followed
611 by 40 cycles of 94 $^{\circ}$ C for 30 s, 55 $^{\circ}$ C for 30 s, and 72 $^{\circ}$ C for 1 min; with a final extension at 72 $^{\circ}$ C
612 for 10 min. The PCR products were purified using the TIANquick Midi Purification Kit (TIANGEN,
613 Beijing, China), and sequenced by Sangon Biotech (Shanghai, China). The resulting nucleotide
614 sequences and their predicted amino acid sequences were aligned and analyzed against the
615 corresponding genes in the reference genome Caméor using DNAMAN v9.0.1.116 (Lynnon Biosoft,
616 PQ, Canada). Moreover, the protein structure of the candidate gene was predicted using the online
617 tool AlphaFold 3 (<https://alphafoldserver.com/>) and visualized with ChimeraX v1.9
618 (<https://www.cgl.ucsf.edu/chimerax/>).

619 **Quantitative real-time PCR (qRT-PCR)**

620 The total RNA was extracted from the roots of parental plants at 0, 12, 24, 48, and 96 h after
621 inoculation, as well as from the root, stem, and leaf tissues of uninoculated parental plants in three
622 biological replicates. Following the manufacturer's protocol, total RNA was extracted with the
623 FastPure Universal Plant Total RNA Isolation Kit (Vazyme Biotech, Nanjing, China) and first-strand
624 cDNA was synthesized using the RT-PCR system for EasyScript First-Strand cDNA Synthesis
625 SuperMix kit (TransGen Biotech, Beijing, China). The qRT-PCR primer pair *PsFwC9*-RT-4F/R for

626 *Psat4g213640* were designed by NCBI primer designing tool and the *PvActin* was employed as an
627 internal control for transcriptional normalization following the recommendations of Die et al. [48]
628 (Table S3). The qRT-PCR reactions were conducted on a QuantStudio™ 5 Real-Time PCR
629 Instrument (Thermo Fisher Scientific, Waltham, MA, USA) with the reaction mixtures: 2 µL cDNA
630 (~ 100 ng/µL), 0.4 µL of each primer, 10 µL 2×*TransStart*® Top Green qPCR SuperMix, and 7.2 µL
631 ddH₂O. The qRT-PCR reactions were performed on an ABI 7500 Real-Time PCR System (Applied
632 Biosystems, USA) using the following program: 50 °C for 2 min; 95 °C for 10 min; followed by 40
633 cycles of 95 °C for 5 s and 60 °C for 34 s. The relative expression levels were calculated and
634 analyzed using the $2^{-\Delta\Delta C_t}$ method [49].

635 ***Agrobacterium rhizogenes*-mediated transformation of seedlings and inoculation**

636 **identification**

637 The full-length cDNA of *PsFwC9* candidate gene *Psat4g213640* was amplified with primer
638 pair OE-*PsFwC9*-F/R (Table S3), incorporating *Nco*I and *Bst*EII restriction sites, and then inserted
639 into the pCAMBIA3301 vector to create the overexpression (OE) vector *PsFwC9*-OE [50]. For
640 RNAi vector, a fragment was sequentially amplified and modified with *Xba*I/*Sma*I and *Spe*I/*Sac*I
641 restriction enzymes, comprising the sense and antisense sequences of *PsFwC9*, and then ligated into
642 the pROKII vector to generate the recombinant RNAi vector *PsFwC9*-RNAi [50]. The
643 pCAMBIA3301 and pROKII vectors were used as controls (CK). The parental lines CW9-1 (for
644 OE) and CW9-8 (for RNAi) were used for transformation with *Agrobacterium rhizogenes* strain
645 K599. Transgenic pea hairy root composite plants were generated using a slightly modified method
646 based on that described by Fan et al. [57] for soybean. After hairy roots developed 14 days, these
647 seedlings with hairy roots were thoroughly washed, with one-third of the hairy roots removed, and
648 then immersed in a microconidia suspension of 1.0×10^7 microconidia/mL. After 24 hours of
649 inoculation, the longest and strongest hairy root, approximately 2 cm in length, was collected from
650 the seedlings. About 1 cm of the collected root was sent to Solabio (Beijing, China) for Periodic
651 acid-Schiff (PAS) staining and the visualization was performed SlideViewer v2.7 software
652 (3DHistech, Budapest, Hungary), while the remainder was used to assess the expression levels of
653 *Psat4g213640*, following the same method as qRT-PCR. The seedlings were then transplanted into
654 new cups for continued observation of their phenotypes. All experiments, including overexpression,
655 gene silencing, and subsequent inoculation, were conducted in three independent biological

656 replicates.

657 **Subcellular localization**

658 The full-length cDNA of *Psat4g213640* in CW9-8, containing *Hind*III and *Spe*I restriction sites,
659 was amplified using the SL-PsFwC9-F/R primer pair (Table S3). The amplified fragment was
660 inserted into the modified pCAMBIA1300-GFP expression vector [50] to generate the
661 35S::PsFwC9^{CW9-8}-GFP and 35S::PsFwC9^{CW9-1}-GFP fusion construct. The recombinant plasmid
662 was introduced into *Agrobacterium tumefaciens* strain GV3101 and used for transient expression in
663 *Nicotiana benthamiana* leaves, with pCAMBIA1300-GFP serving as the control [82]. The tobacco
664 seedlings were kept in the dark for 24 h prior to infiltration, and the leaves were infiltrated with
665 *Agrobacterium* suspensions and incubated for 48 h under suitable growth conditions. Fluorescence
666 signals were observed using an LSM900 confocal laser scanning microscope (Zeiss, Oberkochen,
667 Germany). Based on the preliminary localization pattern observed in the transient expression assay,
668 co-localization analysis was further performed using the corresponding subcellular marker to verify
669 the subcellular localization of *PsFwC9*.

670

ACCEPTED MANUSCRIPT

671 **Acknowledgments**

672 We sincerely thank Professor Dongmei Yu at Sichuan Academy of Agricultural Sciences, Sichuan,
673 China, for providing the lines of Chengwan 9; and Dr. Rebecca J. McGee at Grain Legume Genetics
674 and Physiology Research Unit, USDA ARS, Pullman, WA 99164, USA, for providing the pea
675 differential cultivars. We also sincerely thank Dr. Guangqi Gao at Institute of Crop Sciences,
676 Chinese Academy of Agricultural Sciences, Beijing, China, for providing professional assistance in
677 QTL-seq analyses; Dr. Yonghui Liu, Dr. Mengfei Wang, and Dr. Shuang Wu at Institute of Crop
678 Sciences, Chinese Academy of Agricultural Sciences, Beijing, China, for providing professional
679 assistance in expression analysis, subcellular localization, and overexpression. This study was
680 supported by the China Agriculture Research System of MOF and MARA (CARS-08), the National
681 Key R&D Program of China (2019YFD1001300, 2019YFD1001301), Organization and
682 implementation of crop germplasm resources introduction (22250268), Liaoning Major Science and
683 Technology Special Project (2025JH1/11700019), and the Scientific Innovation Program of the
684 Chinese Academy of Agricultural Sciences.

685

686 **Author contributions**

687 ZZ and SS conceived and designed the experiments. DD, WW, CD, FM, RX, and WG performed
688 the experiments. DD and WW analyzed the data. DD wrote the manuscript. ZZ revised the paper.
689 All authors read and approved the manuscript.

690

691 **Data Availability**

692 The raw sequence data reported in this paper have been deposited in the Genome Sequence Archive
693 (Genomics, Proteomics & Bioinformatics 2025) in National Genomics Data Center (Nucleic Acids
694 Res 2025), China National Center for Bioinformation / Beijing Institute of Genomics, Chinese
695 Academy of Sciences (GSA: CRA033056) that are publicly accessible at
696 <https://ngdc.cncb.ac.cn/gsa>.

697

698 **Conflict of interest**

699 The authors declare that there are no conflicts of interest.

700

701 **Supplementary data**

702 Supplementary data are available at Horticulture Research online.

703 **Fig. S1** Subcellular localization of *PsFwC9* candidate gene *Psat4g213640* in *Nicotiana*
704 *benthamiana* leaves

705 **Table S1** The phenotypic evaluation and diagnostic markers detection in 15 lines of Chengwan 9, 7
706 pea differential cultivars, and 196 accessions

707 **Table S2** The KASP primers for fine mapping

708 **Table S3** List of primers used in study

709 **Table S4** The SNPs and InDels distribution on the seven major chromosomes of the cross between
710 Chengwan 9-1 and Chengwan 9-8

711

ACCEPTED MANUSCRIPT

712 **References**

- 713 [1]. Cousin R. Peas (*Pisum sativum* L.). *Field Crops Res.* 1997; **53**: 111–130.
- 714 [2]. Dahl WJ, Foster LM, Tyler RT. Review of the health benefits of peas (*Pisum sativum* L.). *Br J*
715 *Nutr.* 2012; **108**: S3–S10.
- 716 [3]. Guindon MF, Cazzola F, Palacios T. et al. Biofortification of pea (*Pisum sativum* L.): A review.
717 *J Sci Food Agric.* 2021; **101**: 3551–3563.
- 718 [4]. Wu DT, Li WX, Wan JJ. et al. A comprehensive review of pea (*Pisum sativum* L.): chemical
719 composition, processing, health benefits, and food applications. *Foods.* 2023; **12**: 2527.
- 720 [5]. Li L, Yang T, Liu R. et al. Food legume production in China. *Crop J.* 2017; **5**: 115–126.
- 721 [6]. Woo SL, De Filippis F, Zotti M. et al. Pea-Wheat Rotation Affects Soil Microbiota Diversity,
722 Community Structure, and Soilborne Pathogens. *Microorganisms.* 2022; **10**: 370.
- 723 [7]. Tulbek MC, Wang YL, Hounjet M. Pea—A sustainable vegetable protein crop. In: Sudarshan
724 N, Wanasundara JPD, Scanlin L. et al., eds. *Sustainable Protein Sources*. New York: Academic
725 Press, 2024: 143–162.
- 726 [8]. El-Sharkawy HHA, Abbas MS, Soliman AS. et al. Synergistic effect of growth-promoting
727 microorganisms on bio-control of *Fusarium oxysporum* f. sp. *pisi*, growth, yield, physiological
728 and anatomical characteristics of pea plants. *Pestic Biochem Physiol.* 2021; **178**: 104939.
- 729 [9]. Sharma A, Rathour R, Plaha P. et al. Induction of Fusarium wilt (*Fusarium oxysporum* f. sp.
730 *pisi*) resistance in garden pea using induced mutagenesis and in vitro selection techniques.
731 *Euphytica.* 2010; **173**: 345–356.
- 732 [10]. Deng D, Sun S, Wu W. et al. Screening for pea germplasms resistant to Fusarium wilt race 5.
733 *Agronomy.* 2022; **12**: 1354.
- 734 [11]. Kraft JM, Pflieger FL. *Compendium of Pea Diseases and Pests*, 2nd ed. St. Paul, MN, USA:
735 American Phytopathological Society, 2001: 13–14.
- 736 [12]. Jha UC, Bohra A, Pandey S. et al. Breeding, genetics, and genomics approaches for improving
737 Fusarium wilt resistance in major grain legumes. *Front Genet.* 2020; **11**: 1001.
- 738 [13]. Sampaio AM, Araujo SD, Rubiales D. et al. Fusarium wilt management in legume crops.
739 *Agronomy.* 2020; **10**: 1073.

- 740 [14].Neumann S, Xue AG. Reactions of field pea cultivars to four races of *Fusarium oxysporum* f.
741 *sp. pisi*. *Can J Plant Sci.* 2003; **83**: 377–379.
- 742 [15].Bani M, Rubiales D, Rispaill N. et al. A detailed evaluation method to identify sources of
743 quantitative resistance to *Fusarium oxysporum* f. *sp. pisi* race 2 within a *Pisum* spp. germplasm
744 collection. *Plant Pathol.* 2012; **61**: 532–542.
- 745 [16].Deng D, Sun S, Wu W. et al. Fine mapping and identification of a Fusarium wilt resistance
746 gene *FwSI* in pea. *Theor Appl Genet.* 2024; **137**: 171.
- 747 [17].Jain S, Weeden NF, Kumar A. et al. Functional codominant marker for selecting the *Fw* gene
748 conferring resistance to Fusarium wilt race 1 in pea. *Crop Sci.* 2015; **55**: 2639–2646.
- 749 [18].McPhee KE, Inglis DA, Gundersen B. et al. Mapping QTL for Fusarium wilt race 2 partial
750 resistance in pea (*Pisum sativum*). *Plant Breed.* 2012; **131**: 300–306.
- 751 [19].Kwon SJ, Smýkal P, Hu J. et al. User-friendly markers linked to Fusarium wilt race 1 resistance
752 *Fw* gene for marker-assisted selection in pea. *Plant Breed.* 2013; **132**: 642–648.
- 753 [20].Coyne CJ, Inglis DA, Whitehead SJ. et al. Chromosomal location of *Fwf*, the Fusarium wilt
754 race 5 resistance gene in *Pisum sativum*. *Pisum Genet.* 2000; **32**: 20–22.
- 755 [21].Haglund WA, Kraft JM. *Fusarium oxysporum* f. *sp. pisi*, race 6: Occurrence and distribution.
756 *Phytopathology.* 1979; **81**: 818–820.
- 757 [22].Okubara PA, Inglis DA, Muehlbauer FJ. et al. A novel RAPD marker linked to the Fusarium
758 wilt race 5 resistance gene (*Fwf*) in *Pisum sativum*. *Pisum Genet.* 2002; **34**: 6–8.
- 759 [23].Rozhmina TA, Kanapin AA, Bankin MP. et al. Identification of two QTLs controlling flax
760 resistance to Fusarium wilt. *Biophysics.* 2024; **81**: 57–62.
- 761 [24].Tassone MR, Bagnaresi P, Desiderio F. et al. A genomic BSA-seq approach for the
762 characterization of QTLs underlying resistance to *Fusarium oxysporum* in eggplant. *Cells.*
763 2022; **11**: 2548.
- 764 [25].Van Ooijen G, Mayr G, Kasiem MM. et al. Structure-function analysis of the NB-ARC domain
765 of plant disease resistance proteins. *J Exp Bot.* 2008; **59**: 1383–1397.
- 766 [26].Shokouhifar F, Mamarabadi M, Khyrabad MM. et al. Tracking of the gene *Fom2* and study on
767 the genetic diversity of NB-ARC domain in the number of resistant and sensitive melon
768 cultivars against *Fusarium oxysporum* f. *sp. melonis* (race 1). *Australas Plant Pathol.* 2016; **45**:
769 279–288.

- 770 [27].Wu X, Li N, Hao J. et al. Genetic diversity of Chinese and global pea (*Pisum sativum L.*)
771 collections. *Crop Sci.* 2017; **57**: 1574–1584.
- 772 [28].Chen HL, Tian J, Zhu ZD. et al. Current status and future prospective of food legumes
773 production and seed industry in China. *Sci Agric Sin.* 2021; **54**: 493–503 (In Chinese).
- 774 [29].FAO (Food and Agriculture Organization). Online statistical database: Crops and livestock
775 products. <https://www.fao.org/faostat/en/#data/QCL>, 2023 (accessed 11 June 2025).
- 776 [30].Zhang J. Rates of conservative and radical nonsynonymous nucleotide substitutions in
777 mammalian nuclear genes. *J Mol Evol.* 2000; **50**: 56–68.
- 778 [31].Wang M, Wang D, Yu J. et al. Enrichment in conservative amino acid changes among fixed
779 and standing missense variations in slowly evolving proteins. *PeerJ.* 2020; **8**: e9983.
- 780 [32].Michielse CB, Rep M. Pathogen profile update: *Fusarium oxysporum*. *Mol Plant Pathol.* 2009;
781 **10**: 311.
- 782 [33].Ma LJ, Van Der Does HC, Borkovich KA. et al. Comparative genomics reveals mobile
783 pathogenicity chromosomes in *Fusarium*. *Nature.* 2010; **464**: 367–373.
- 784 [34].Taylor A, Vágány V, Jackson AC. et al. Identification of pathogenicity-related genes in
785 *Fusarium oxysporum* f. sp. *cepae*. *Mol Plant Pathol.* 2016; **17**: 1032–1047.
- 786 [35].Dita M, Barquero M, Heck D. et al. Fusarium wilt of banana: current knowledge on
787 epidemiology and research needs toward sustainable disease management. *Front Plant Sci.*
788 2018; **9**: 1468.
- 789 [36].Joshi RK, Nayak S. Gene pyramiding—A broad spectrum technique for developing durable
790 stress resistance in crops. *Biotechnol Mol Biol Rev.* 2010; **5**: 51–60.
- 791 [37].Dormatey R, Sun C, Ali K. et al. Gene pyramiding for sustainable crop improvement against
792 biotic and abiotic stresses. *Agronomy.* 2020; **10**: 1255.
- 793 [38].Michelmore RW, Paran I, Kesseli RV. Identification of markers linked to disease-resistance
794 genes by bulked segregant analysis: a rapid method to detect markers in specific genomic
795 regions by using segregating populations. *Proc Natl Acad Sci USA.* 1991; **88**: 9828–9832.
- 796 [39].Takagi H, Abe A, Yoshida K. et al. QTL-seq: rapid mapping of quantitative trait loci in rice
797 by whole genome resequencing of DNA from two bulked populations. *Plant J.* 2013; **74**: 174–
798 183.

- 799 [40]. Sugihara Y, Young L, Yaegashi H. et al. High-performance pipeline for MutMap and QTL-
800 seq. *PeerJ*. 2022; **10**: e13170.
- 801 [41]. Rubiales D, González-Bernal MJ, Warkentin T. et al. Advances in pea breeding. In: Hochmuth
802 G, ed. *Achieving Sustainable Cultivation of Vegetables*. Cambridge, UK: Burleigh Dodds
803 Science Publishing, 2019: 575–606.
- 804 [42]. Zhang B, Qi F, Hu G. et al. BSA-seq-based identification of a major additive plant height QTL
805 with an effect equivalent to that of Semi-dwarf 1 in a large rice F2 population. *Crop J*. 2021;
806 **9**: 1428–1437.
- 807 [43]. Wang Y, Teng Z, Li H. et al. An activated form of NB-ARC protein *RLSI* functions with
808 cysteine-rich receptor-like protein *RMC* to trigger cell death in rice. *Plant Commun*. 2023; **4**:
809 100459.
- 810 [44]. Beniwal D, Dhall RK, Vikal Y. et al. BSA-seq identifies a major locus on chromosome-6 for
811 rust (*Uromyces viciae-fabae*) resistance in garden pea (*Pisum sativum* L.). *Nucleus*. 2024; **1**:
812 1–11.
- 813 [45]. Beji S, Fontaine V, Devaux R. et al. Genome-wide association study identifies favorable SNP
814 alleles and candidate genes for frost tolerance in pea. *BMC Genomics*. 2020; **21**: 1–21.
- 815 [46]. Zheng Y, Xu F, Li Q. et al. QTL mapping combined with bulked segregant analysis identify
816 SNP markers linked to leaf shape traits in *Pisum sativum* using SLAF sequencing. *Front Genet*.
817 2018; **9**: 615.
- 818 [47]. Zhang P, Wang Y, Sun T. et al. Fine mapping *PsPS1*, a gene controlling pod softness that
819 defines market type in pea (*Pisum sativum*). *Plant Breed*. 2022; **141**: 418–428.
- 820 [48]. Die JV, Román B, Nadal S. et al. Evaluation of candidate reference genes for expression studies
821 in *Pisum sativum* under different experimental conditions. *Planta*. 2010; **232**: 145–153.
- 822 [49]. Livak KJ, Schmittgen TD. Analysis of relative gene expression data using real-time
823 quantitative PCR and the $2^{-\Delta\Delta Ct}$ method. *Methods*. 2001; **25**: 402–408.
- 824 [50]. Wu L, Chang Y, Wang L. et al. The aquaporin gene *PvXIP1;2* conferring drought resistance
825 identified by GWAS at seedling stage in common bean. *Theor Appl Genet*. 2022; **135**: 485–
826 500.
- 827 [51]. Schmittgen TD, Livak KJ. Analyzing real-time PCR data by the comparative CT method. *Nat*
828 *Protoc*. 2008; **3**: 1101–1108.

- 829 [52]. Ye J, Jin CF, Li N. et al. Selection of suitable reference genes for qRT-PCR normalisation
830 under different experimental conditions in *Eucommia ulmoides* Oliv. *Sci Rep.* 2018; **8**: 15043.
- 831 [53]. Bartholomew ES, Xu S, Zhang Y. et al. A chitinase *CsChi23* promoter polymorphism underlies
832 cucumber resistance against *Fusarium oxysporum* f. sp. *cucumerinum*. *New Phytol.* 2022; **236**:
833 1471–1486.
- 834 [54]. Dong C, Zhang L, Zhang Q. et al. *Tiller Number1* encodes an ankyrin repeat protein that
835 controls tillering in bread wheat. *Nat Commun.* 2023; **14**: 836.
- 836 [55]. Huang S, Wang J, Song R. et al. Balanced plant helper NLR activation by a modified host
837 protein complex. *Nature.* 2025; **1**: 1–9.
- 838 [56]. Miao P, Wang H, Wang W. et al. A widespread plant defense compound disarms bacterial type
839 III injectisome assembly. *Science.* 2025; **387**: eads0377.
- 840 [57]. Fan YL, Zhang XH, Zhong LJ. et al. One-step generation of composite soybean plants with
841 transgenic roots by *Agrobacterium rhizogenes*-mediated transformation. *BMC Plant Biol.* 2020;
842 **20**: 208.
- 843 [58]. Kereszt A, Li D, Indrasumunar A. et al. *Agrobacterium rhizogenes*-mediated transformation
844 of soybean to study root biology. *Nat Protoc.* 2007; **2**: 948–952.
- 845 [59]. Georgiev M, Agostini E, Ludwig-Müller J. et al. Genetically transformed roots: from plant
846 disease to biotechnological resource. *Trends Biotechnol.* 2012; **30**: 528–537.
- 847 [60]. Yu WC, Fersht AR. Stability and solvation of Thr/Ser to Ala and Gly mutations at the N-cap
848 of α -helices. *FEBS Lett.* 1994; **347**: 304–309.
- 849 [61]. Wang W, Hu B, Li A. et al. *NRT1.1s* in plants: functions beyond nitrate transport. *J Exp Bot.*
850 2020; **71**: 4373–4379.
- 851 [62]. Sun J, Bankston JR, Payandeh J. et al. Crystal structure of the plant dual-affinity nitrate
852 transporter *NRT1.1*. *Nature* 2014; **507**: 73–77.
- 853 [63]. Liu KH, Liu M, Lin Z. et al. NIN-like protein 7 transcription factor is a plant nitrate sensor.
854 *Science.* 2022; **377**: 1419–1425.
- 855 [64]. Nguyen TA, Lee C. Thr-to-Ala mutation leads to a larger aromatic pair and reduced packing
856 density in $\alpha 1$, $\alpha 3$ -helices during thioredoxin cold adaptation. *ACS Omega.* 2024; **9**: 10812–
857 10824.
- 858 [65]. Eichmann R, Schäfer P. The endoplasmic reticulum in plant immunity and cell death. *Front*

- 859 *Plant Sci.* 2012; **3**: 200.
- 860 [66]. Saijo Y. ER quality control of immune receptors and regulators in plants. *Cell Microbiol.* 2010;
861 **12**: 716–724.
- 862 [67]. Bi W, Chen Y, Song Y. et al. Potato DMP2 positively regulates plant immunity by modulating
863 endoplasmic reticulum homeostasis. *J Integr Plant Biol.* 2025; **67**: 1568–1581.
- 864 [68]. Groenendyk J, Agellon LB, Michalak M. Calcium signaling and endoplasmic reticulum stress.
865 *Int Rev Cell Mol Biol.* 2021; **363**: 1–20.
- 866 [69]. Krebs J, Agellon LB, Michalak M. Ca²⁺ homeostasis and endoplasmic reticulum (ER) stress:
867 An integrated view of calcium signaling. *Biochem Biophys Res Commun.* 2015; **460**: 114–121.
- 868 [70]. Cao J, Wang C, Hao N. et al. Endoplasmic reticulum stress and reactive oxygen species in
869 plants. *Antioxidants.* 2022; **11**: 1240.
- 870 [71]. Eisner V, Csordás G, Hajnóczky G. Interactions between sarco-endoplasmic reticulum and
871 mitochondria in cardiac and skeletal muscle—pivotal roles in Ca²⁺ and reactive oxygen species
872 signaling. *J Cell Sci.* 2013; **126**: 2965–2978.
- 873 [72]. Chen S, Zhou Y, Chen Y. et al. fastp: an ultra-fast all-in-one FASTQ preprocessor.
874 *Bioinformatics.* 2018; **34**: i884–i890.
- 875 [73]. Vasimuddin M, Misra S, Li H. et al. Efficient architecture-aware acceleration of BWA-MEM
876 for multicore systems. In: *Proceedings of the 2019 IEEE International Parallel and Distributed
877 Processing Symposium (IPDPS)*. Rio de Janeiro, Brazil, 2019: 314–324.
- 878 [74]. Kreplak J, Madoui MA, Cápál P. et al. A reference genome for pea provides insight into legume
879 genome evolution. *Nat Genet.* 2019; **51**: 1411–1422.
- 880 [75]. Danecek P, Bonfield JK, Liddle J. et al. Twelve years of SAMtools and BCFtools. *Gigascience.*
881 2021; **10**: giab008.
- 882 [76]. Van der Auwera GA, O'Connor BD. *Genomics in the Cloud: Using Docker, GATK, and WDL
883 in Terra*. Sebastopol, CA, USA: O'Reilly Media, 2020.
- 884 [77]. Poplin R, Ruano-Rubio V, DePristo MA. et al. Scaling accurate genetic variant discovery to
885 tens of thousands of samples. *bioRxiv.* 2017; 201178.
- 886 [78]. Danecek P, Auton A, Abecasis G. et al. The variant call format and VCFtools. *Bioinformatics.*
887 2011; **27**: 2156–2158.

- 888 [79].Cingolani P, Platts A, Wang LL. et al. A program for annotating and predicting the effects of
889 single nucleotide polymorphisms, SnpEff: SNPs in the genome of *Drosophila melanogaster*
890 strain w1118; iso-2; iso-3. *Fly*. 2012; **6**: 80–92.
- 891 [80].Chen C, Wu Y, Li J. et al. TBtools-II: A “one for all, all for one” bioinformatics platform for
892 biological big-data mining. *Mol Plant*. 2023; **16**: 1733–1742.
- 893 [81].Wood DE, Lu J, Langmead B. Improved metagenomic analysis with Kraken 2. *Genome Biol*.
894 2019; **20**: 257.
- 895 [82].Sheludko YV, Sindarovska YR, Gerasymenko IM. et al. Comparison of several *Nicotiana*
896 species as hosts for high-scale *Agrobacterium*-mediated transient expression. *Biotechnol*
897 *Bioeng*. 2007; **96**: 608–614.

ACCEPTED MANUSCRIPT